

## NUMERICAL INVESTIGATION OF AN R744 LIQUID EJECTOR FOR SUPERMARKET REFRIGERATION SYSTEMS

by

**Michał HAIDA<sup>a</sup>, Jacek SMOLKA<sup>a\*</sup>, Michał PALACZ<sup>a</sup>, Jakub BODYS<sup>a</sup>,  
Andrzej J. NOWAK<sup>a</sup>, Zbigniew BULINSKI<sup>a</sup>, Adam FIC<sup>a</sup>, Krzysztof BANASIAK<sup>b</sup>,  
and Armin HAFNER<sup>b</sup>**

<sup>a</sup> Institute of Thermal Technology, Silesian University of Technology, Gliwice, Poland

<sup>b</sup> SINTEF Energy Research, Trondheim, Norway

Original scientific paper

DOI: 10.2298/TSCI151210112H

*This paper presents a numerical investigation of an R744 liquid ejector applied to a supermarket refrigeration system. The use of the liquid ejector enables the operation of the evaporator in a flooded mode and recirculates the R744 liquid phase, which improves the energy efficiency of the refrigeration system. The investigation was performed using two ejectors of different sizes installed in a multi-ejector block. The numerical model was formulated based on the homogenous equilibrium model and validated with the experimental results. The influence of the pre-mixer, mixer and diffuser dimensions on the ejector performance measured using the mass entrainment ratio is presented. The results show that the best liquid ejector performance was obtained for the short lengths of the pre-mixer and mixer compared to the broadly investigated two-phase ejectors connected to the evaporator port. In addition, wide diffuser angles improved the mass entrainment ratio of both liquid ejectors, which may lead to a reduction in the diffuser length.*

Key words: *liquid ejector, fixed ejector, homogeneous equilibrium model, CO<sub>2</sub>, R744, refrigeration system*

### Introduction

Carbon dioxide, as a natural refrigerant with a neutral impact on the global warming potential and non-ozone depletion potential, is one of the most popular refrigerants applied in modern supermarket refrigeration systems. CO<sub>2</sub> refrigeration systems are commonly installed in cold climates as a result of the significant system energy performance degradation experienced when the ambient temperature is higher than the CO<sub>2</sub> critical temperature of 30.98 °C. However, the use of a two-phase ejector as an expansion device in recent R744 transcritical refrigeration systems has improved the coefficient of performance (COP), as discussed in the recent literature [1-5]. Hence, the ejector technology can expand the application area of R744 refrigeration systems into warm climates to be more competitive.

The development of devices implemented in refrigeration units improves the energy efficiency of refrigeration systems. An ejector used as an expansion device represents a method for increasing the system COP. In a typical refrigeration cycle, the throttling process produces large energy losses due to the irreversible isenthalpic expansion process. An ejector

\* Corresponding author; e-mail: jacek.smolka@polsl.pl

applied to the system can recover some of this energy loss as a result of the entrainment of the low-pressure stream by the high-pressure motive stream under isentropic conditions [6].

Apart from the application of a two-phase ejector as an expansion device, the implementation of a liquid ejector can also improve the energy efficiency of a refrigeration system. In a standard vapour compression cycle, the evaporator is set with the assumed superheat to provide the vapour phase of the refrigerant on the suction side of the compressors [7]. However, the application of the liquid ejector together with the accumulator tank outside of the evaporator enables the ability to completely fill the evaporator with the liquid refrigerant, thereby omitting the superheating of the refrigerant. The flooded evaporator improves the heat transfer coefficient and increases the mass flow rate of the flowing refrigerant through the evaporator. The accumulator tank ensures that the saturated vapour refrigerant in the compressor rack and the saturated liquid are entrained by the liquid ejector. The benefit of using the liquid ejector in the re-circulation of the saturated liquid refrigerant is its simple geometry, lack of moving parts and consequently significantly lower production cost compared to that of a liquid pump [7, 8].

The improved energy efficiency of a refrigeration system that uses the liquid ejector has been demonstrated in the literature. In the paper [7], an R134a liquid ejector was experimentally investigated. The ejector was installed in a horizontal-tube falling-film evaporator. The authors stated that gradually increasing the motive flow rate in the liquid ejector increased the evaporating capacity by up to 4.8% and the COP of the refrigeration by up to 2.3% for a recirculation ratio of 1.135.

The experimental analysis of the liquid ejector as a re-circulator component in an overfeed plate evaporator with ammonia was performed in the paper [8]. The test facility consisted of an R744 low-temperature cycle, NH<sub>3</sub> medium-temperature cycle with an air condenser, an ammonia compressor, a separator, a liquid ejector and a cascade overfeed NH<sub>3</sub> evaporator. The experimental results indicated that the re-circulated liquid volumetric flow rate tended to decrease with increasing motive mass flow rate in the liquid ejector. When the ammonia condensing pressure increased, the liquid re-circulated volumetric flow rate as well as the recirculation rate increased.

The R744 supermarket refrigeration system equipped with the liquid ejector has already been manufactured and installed in commercial supermarkets [9, 10]. The liquid ejector maintained a constant temperature throughout the evaporator, which allowed the increase in the evaporation temperature. The author stated that, for an average increase in the evaporation temperature of 5 K, the energy consumption of the refrigeration system was reduced by approximately 15% throughout the year. In addition, the increased evaporation temperature reduced the pressure ratio of the compressor.

According to the best knowledge of the authors, the numerical investigation of the R744 liquid ejector has not been published yet. Therefore, the objective of this paper is to numerically analyse two R744 liquid ejectors with different sizes as a re-circulating component in the R744 refrigeration system. Both investigated liquid ejectors are implemented into the multi-ejector expansion work recovery pack applied in the R744 supermarket refrigeration system [11]. The employed numerical model is based on the homogenous equilibrium model (HEM) described in detail in [12] and later fully validated in [13]. In all the simulations, the *ejectorPL* platform was used to analyse the considered cases in a controlled and systematic manner [13]. The numerical results were validated with the experimental results obtained on a test rig designed for multi-ejector testing purposes at the SINTEF Energy Research laboratory in Trondheim, Norway [11]. Then, a sensitivity analysis of the liquid ejector geometry param-

eters on the device performance was performed and discussed. Namely, the pre-mixer length, the mixer length and diameter and the diffuser angle were investigated, therein showing a large influence on the obtained mass entrainment ratio.

### Application of the liquid ejectors

The liquid ejector mixes two streams with different parameters. The high-pressure flow, after being subject to heat rejection in the gas cooler section, is subcooled and flows through the motive nozzle. In the suction nozzle, the entrained flow is a saturated liquid with a pressure equal to the evaporation pressure in the medium-temperature evaporator. The liquid receiver tank installed behind the evaporator allows the evaporator to operate in the flooded mode and provides the liquid flow to the suction port of the ejector.

The motive fluid flows through the converging-diverging nozzle, where the enthalpy is transformed into kinetic energy. Hence, the pressure of the motive fluid decreases, and in the throat, the velocity of the fluid achieves to the speed of sound. Then, the supersonic motive stream mixes and exchanges momentum with the low-pressure suction stream in the pre-mixing and mixing sections, resulting in a mixture with increased pressure. The high kinetic energy of the mixed flow is converted to pressure in the diffuser. Therefore, the pressure increases along the increasing cross-sectional area of the diffuser. Finally, the mixed stream flows through the outlet port to the receiver tank.

The general purpose of the liquid ejector in refrigeration is to maximise the recirculation of the liquid refrigerant between the two tanks. The motive high-pressure supersonic flow entrains and mixes with the suction low-pressure liquid flow. Finally, the mixed flow exits the ejector as the intermediate-pressure flow. Therefore, the performance of the liquid ejector is mainly described by the mass entrainment ratio, which is the ratio between the mass flow rate of the suction stream and that of the motive stream.

$$\phi = \frac{\dot{m}_{\text{suction}}}{\dot{m}_{\text{motive}}} \quad (1)$$

where  $\phi$  is the mass entrainment ratio and  $\dot{m}_{\text{suction}}$  and  $\dot{m}_{\text{motive}}$  are the suction nozzle and motive nozzle mass flow rates, respectively.

### Liquid ejector design and operating conditions

In this paper, the two R744 liquid ejectors applied in the R744 supermarket refrigeration system were investigated. Both ejectors were designed for different refrigeration system loads. The capacity of the ejector EJ1 was two-times smaller than the capacity of the ejector EJ2. Figure 1 presents the shape and dimensions of the R744 liquid ejector. The configuration of both liquid ejectors was comparable to that of the vapour ejectors applied in [4]. The considered liquid ejector consisted of five main sections: motive nozzle, suction nozzle, pre-mixer, mixer and diffuser.

Table 1 presents the dimensions of both liquid ejectors. The motive nozzle of the ejector EJ1 was smaller than that of the ejector EJ2. The difference in the throat diameter resulted in the maximum possible motive mass flow rate of CO<sub>2</sub>. Hence, EJ2 obtained two-times higher mass flow rates than did EJ1. Moreover, the mixer and pre-mixer lengths of EJ2 are longer than those of EJ1.

To validate the numerical model of the R744 liquid ejector, the experimental investigation was conducted at the SINTEF Energy Research Laboratory in Trondheim, Norway. The test facility was designed and manufactured to map the performance of the R744 vapour

and liquid ejectors in the multi-ejector module, which was shown and described in detail in [11]. Table 2 presents the experimentally obtained operating conditions of EJ1 and EJ2 corresponding to the supermarket refrigeration application. The inlet motive nozzle parameters were in the transcritical mode, where the highest pressure was 87.75 bar. The difference between the outlet pressure and the suction pressure was in the range of 4.21 bar to 7.24 bar. The suction nozzle parameters corresponded to a saturated liquid at an evaporation temperature between  $-3.9\text{ }^{\circ}\text{C}$  and  $-8.9\text{ }^{\circ}\text{C}$ . The liquid  $\text{CO}_2$  on the suction side was transferred from the bottom connector of the liquid receiver. The receiver was equipped with an R744 liquid level sensor to ensure that the liquid ejector was removing the saturated  $\text{CO}_2$  liquid. The motive stream, following the heat rejection process in the gas cooler sections, was subcooled in the additional internal heat exchangers to improve the ejectors' performance. Moreover, the motive nozzle of each ejector was equipped with a solenoid valve to control the overall capacity of the multi-ejector module. The outlet collector of the module was connected to the receiver tank, thereby allowing the pressure level of the motive, suction and outlet side of the ejectors to be set by the controller. In addition, the receiver tank ensured that the R744 liquid and vapour phases remained in saturation.

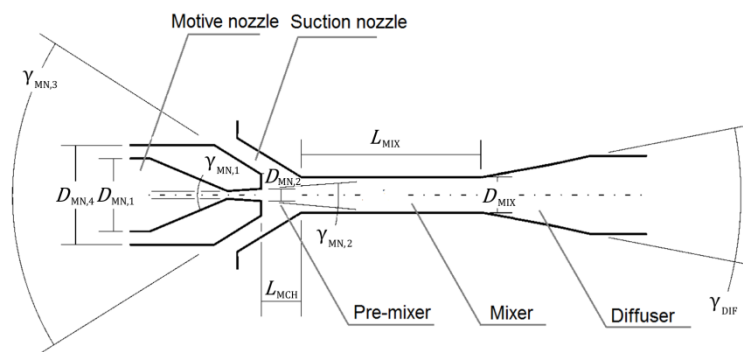


Figure 1. Shape and dimensions of the R744 liquid ejector

Table 1. Geometry of the considered liquid ejectors

Parameter name	Symbol	Unit	EJ1	EJ2
Motive nozzle inlet diameter	$D_{MN,1}$	mm	3.80	3.80
Motive nozzle outlet diameter	$D_{MN,2}$	mm	1.12	1.58
Motive nozzle converging angle	$\gamma_{MN,1}$	$^{\circ}$	30.00	30.00
Motive nozzle diverging angle	$\gamma_{MN,2}$	$^{\circ}$	2.00	2.00
Motive nozzle outer angle	$\gamma_{MN,3}$	$^{\circ}$	38.00	38.00
Pre-Mixer length	$L_{MCH}$	mm	2.70	3.70
Mixer length	$L_{MIX}$	mm	11.50	16.25
Mixer diameter	$D_{MIX}$	mm	2.30	3.25
Diffuser angle	$\gamma_{DIFF}$	$^{\circ}$	5.00	5.00

The test facility was fully controlled by the set of the sensors connected to a controller system. The temperature was measured by PT1000 calibrated thermocouples, which have an accuracy of  $\pm 0.6\text{ K}$ . In addition to the thermocouples, the test rig was equipped with calibrated piezoelectric elements for the pressure measurements and calibrated Coriolis type mass flow meters with an accuracy of  $\pm 2.5 \cdot 10^{-4}\text{ Pa}$  and  $\pm 0.5 \cdot 10^{-3}\text{ kg/s}$ .

**Table 2. Set of operating conditions taken from the experimental results**

Liquid ejector	Case	Motive nozzle		Suction nozzle		Outlet	Mass entrainment ratio
		Pressure	Temperature	Pressure	Quality	Pressure	
		[bar]	[°C]	[bar]	[-]	[bar]	
EJ1	#1.1	75.60	27.7	30.11	0.0	35.80	1.20
	#1.2	85.84	27.9	28.15	0.0	33.87	0.77
	#1.3	87.75	31.7	27.92	0.0	34.84	0.94
	#1.4	79.54	26.0	29.53	0.0	35.19	0.92
	#1.5	86.36	28.7	27.91	0.0	32.85	0.78
	#1.6	87.48	29.2	28.21	0.0	32.89	0.81
EJ2	#2.1	79.51	25.8	29.01	0.0	35.42	1.00
	#2.2	85.61	28.3	27.67	0.0	31.88	0.91
	#2.3	85.39	32.4	27.62	0.0	34.86	1.23
	#2.4	75.50	26.4	27.35	0.0	32.85	1.17
	#2.5	75.72	25.8	31.41	0.0	36.77	1.28
	#2.6	85.74	27.8	27.53	0.0	33.89	0.87

### Computational tool

The mathematical model of a transcritical compressible flow of R744 in the investigated liquid ejectors was based on the HEM approach [14] for a two-phase flow. The HEM model assumes that pressure, temperature, turbulence kinetic energy, turbulence dissipation rate and velocity for both phases of the fluid are equal. Therefore, the energy equation is defined according to the enthalpy-based formulation, and the fluid properties are modelled as a function of specific enthalpy and pressure. The HEM applied to a 3-D model of the R744 ejector was described and experimentally validated in [12].

The validation of the HEM approach for a broad range of operating conditions of the R744 two-phase ejector was presented in [13]. The authors stated that the accuracy of the HEM in comparison to experimental data guarantees high accuracy for the high motive nozzle inlet pressure over the critical point of CO<sub>2</sub> and for the motive nozzle inlet temperature close to the critical temperature of CO<sub>2</sub>. Hence, the set of operating conditions for the motive nozzle inlet parameter presented in this paper were validated in [13]. The real fluid properties of R744 were approximated based on data obtained using the REFPROP libraries [15]. The realisable *k-ε* model was used to model the turbulent flow inside the ejector.

The numerical investigation was performed using the commercial ANSYS software with the *ejectorPL* platform [13]. The purpose of the *ejectorPL* software is to automate the simulation process by combining and controlling the geometry together with the mesh generator ANSYS ICEM CFD, executing the solver in ANSYS Fluent for the flow simulation, and finally processing the data for the ejector operation. The 2-D axisymmetric ejector geometry was discretised with a fully structured grid of less than 10,000 elements with a minimum orthogonal quality of 0.9.

### Results and discussion

#### *Validation of the CFD liquid ejector model*

Figure 2 shows the motive and the suction mass flow rates of EJ1 obtained by the numerical model in comparison to the experimental results. The motive mass flow rate obtained in the experimental work was larger than that obtained from the CFD model results. In the case of the suction mass flow rate, the experimental results indicated a smaller entrain-

ment, aside from case #1.3. The maximum error of the motive mass flow rate for the CFD results was approximately 13%. The average discrepancy of the motive mass flow rate was approximately 11%, which showed a constant decrease in the motive mass flow rate obtained from the CFD results. For the suction mass flow rates, the maximum and average discrepancies between both methods were 23% and 10%, respectively. The agreement of both mass flow rates obtained from the CFD results in comparison to the experimental work were very satisfactory under the considered operating conditions.

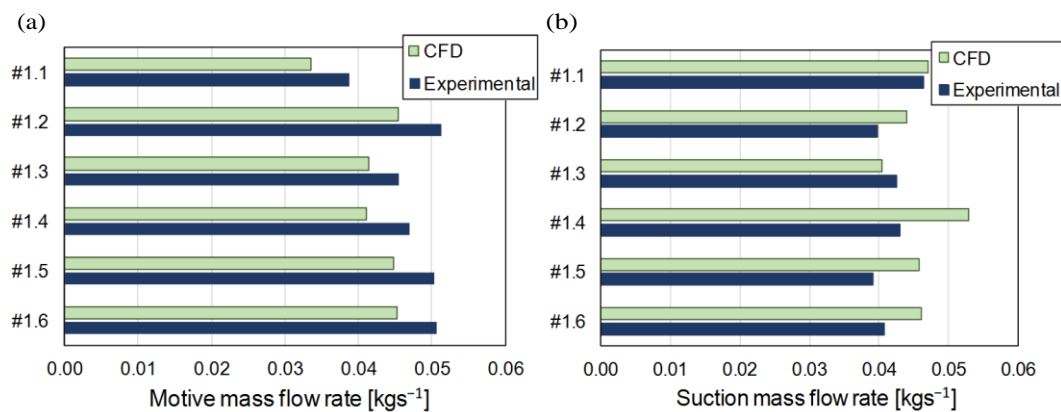


**Figure 2. CFD vs. experimental results of the EJ1 suction mass flow rate (a) and the motive mass flow rate (b)**

Figure 3 presents the EJ2 motive and suction mass flow rate comparison similar to that in fig. 2. As in the case of the smaller ejector EJ1, the discrepancy between the numerical and experimental results for all cases was much smaller. The average discrepancy of the motive nozzle was approximately 5%, and the maximum error was approximately 9%. Therefore, the results for EJ2 obtained based on the CFD results indicated higher accuracy than the results for EJ1. Similarly to the motive mass flow, the discrepancy in the suction mass flow rate for EJ2 was lower than the discrepancy in the EJ1 suction mass flow rate. The average value was approximately 3%.

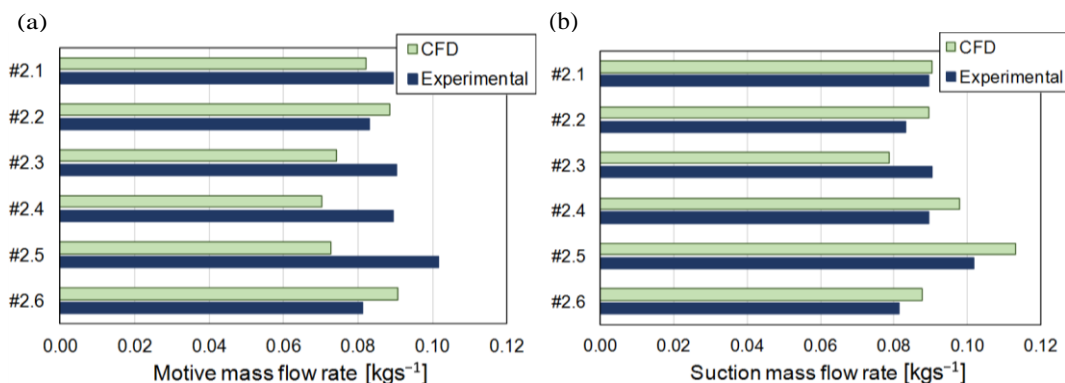


**Figure 3. CFD vs. experimental results of the EJ2 suction mass flow rate (a) and the motive mass flow rate (b)**

However, the highest discrepancy of approximately 13% was observed for the over-estimated mass flow rate in the suction nozzle, which occurred under operating condition #2.3 only. The small errors between both mass flow rates influenced the high accuracy of the liquid ejector performance obtained from the CFD results in comparison with the experimental work. Hence, the mass entrainment ratio for the CFD results differed from the experimental results by on average 10%.

#### *Performance characteristics of the R744 liquid ejector*

Information about the specific parameter distribution within the liquid ejector allowed us to find areas of the device where potential optimisation could be performed to improve the performance of the ejector. Figure 4 presents the EJ2 distributions of pressure, Mach number and vapour quality under operating conditions #2.1. The motive stream significantly expanded through the converging-diverging nozzle due to the transformation of enthalpy into kinetic energy. Therefore, the motive flow indicated a maximum Mach number of 1.5 in the pre-mixer. The shockwaves of the supersonic motive flow occurred in the pre-mixer section. They caused a decrease in pressure to the lower value compared to the pressure of the suction stream. As the pressure of the motive stream decreased, the vapour quality of the flow increased slightly after the throat. Therefore, the motive flow entered the pre-mixer as a two-phase flow. In the mixer, the suction liquid flow mixed with the supersonic motive flow, and the vapour quality stabilised. The non-mixed suction liquid flowed over the mixed flow along the diffuser, where the kinetic energy was used to produce the higher pressure. Finally, the outlet flow indicated a vapour quality of less than 0.4.

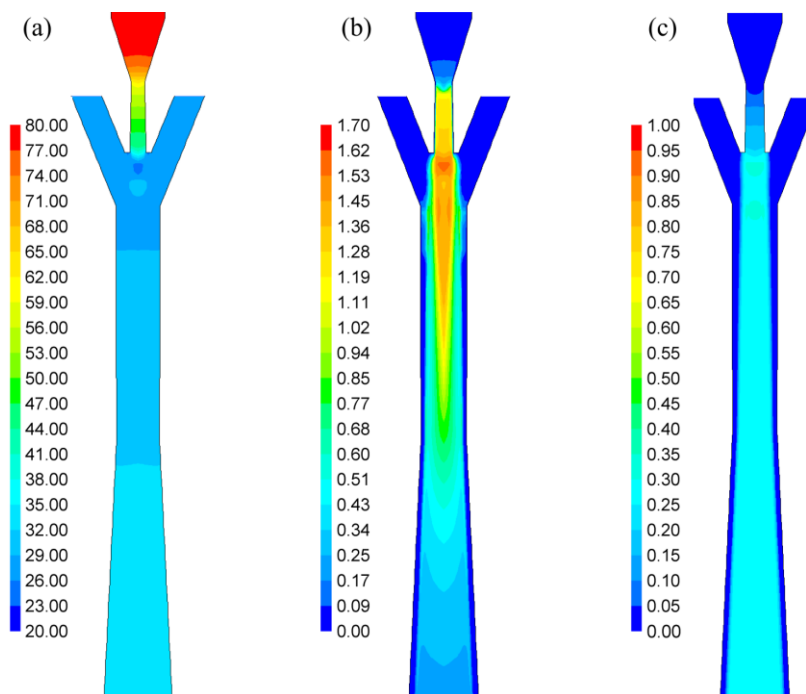


**Figure 4. Contour plots of EJ2 under operating conditions #2.1: pressure (a), Mach number (b), vapour quality (c)**

*The sensitivity analysis based on the parameterisation procedure*

Table 3 presents a set of selected ejector dimensions, which were varied to investigate their influence on the performance of the liquid ejector. The parameterisation concerned the pre-mixer length, the mixer length and diameter and the diffuser angle. The ranges of the pre-mixer length and the mixer diameter for both ejectors were independently defined due to different sizes of the motive nozzles.

**Table 3. The parameterisation range for the EJ1 and EJ2 geometries**

Parameter name	EJ1	EJ2
Pre-mixer length [mm]	1.7; 2.0; 2.2; 2.4; 2.7; 3.2	2.6; 2.9; 3.2; 3.4; 3.7; 4.2
Mixer length [mm]	from 4.5 to 12.5 Step 1.0	from 4.5 to 12.5 Step 1.0
Mixer diameter [mm]	from 2.2 to 2.4 Step 0.1	from 3.15 to 3.35 Step 0.1
Diffuser angle [°]	from 2.5 to 15.0 Step 2.5	from 2.5 to 15.0 Step 2.5

The parameterisation procedure was performed under the same operating conditions #1.3 for EJ1 and operating conditions #2.3 for EJ2. Only one set of operating conditions for each ejector was used because both investigated liquid ejectors were in agreement with CFD predictions. This observation was in contrast to the vapour ejector operation, which was presented in [12]. The mass entrainment ratios were compared to present the influence of the selected dimension change on the liquid ejector performance. As a result of the fixed parameters at the motive nozzle inlet, the motive mass flow rate was constant, and the value of the mass entrainment ratio only depended on the value of the suction mass flow rate. The baseline mass entrainment ratios of EJ1 and EJ2 for all the considered conditions were 0.97 and 1.06, respectively.

Figure 5 presents the sensitivity analysis of the pre-mixer length. The mass entrainment improvement is presented for EJ1 and EJ2. Note that, for both ejectors, the mass entrainment ratio increased with decreasing pre-mixer length.

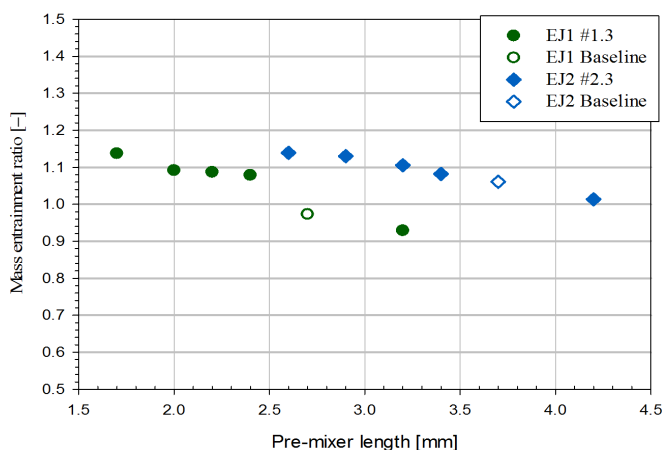
**Figure 5. Mass entrainment ratio vs. pre-mixer length for EJ1 and EJ2**

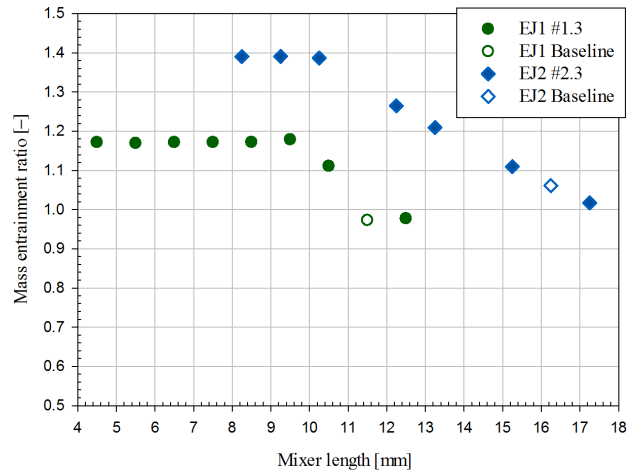
Figure 5 presents the sensitivity analysis of the pre-mixer length. The mass entrainment ratio increased with decreasing pre-mixer length. EJ1 improved the mass entrainment ratio by up to 17% for a pre-mixer length of 1.7 mm, which caused a reduction in the pre-mixer length of 1 mm. Relative to EJ1, the mass entrainment improvement of EJ2 was 7% for the shorter pre-mixer length of 2.6 mm. The reduction in the EJ2 pre-mixer length indicated equalisation of the mass entrainment ratio. Hence, the optimisation of the pre-mixer length can be performed to determine the best improvement.



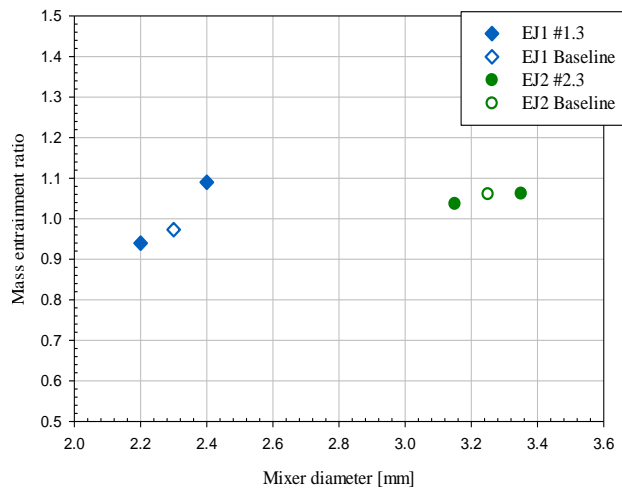
The same trend of the mass entrainment improvement for the short pre-mixer was observed for the shorter mixer section, as presented in fig. 6. For the mixer length of 9.5 mm, EJ1 indicated the best mass entrainment ratio improvement of 31%. However, the mass entrainment ratio was slightly lower for the mixer length in the range of 4.5 mm to 8.5 mm. Hence, the optimum point for the EJ1 mixer length was found. Relative to EJ1, EJ2 also obtained the optimum point for a similar mixer length. In the case of EJ2, the mass entrainment improvement was 31% for a mixer length of 9.25 mm, which was much greater than that of EJ1.

Figure 7 presents the mass entrainment ratio of EJ1 and EJ2 as a function of the mixer diameter. EJ1 indicated the best performance for a mixer diameter of 2.4 mm, and the mass entrainment ratio improvement was 12%. For EJ2, the increase in the mixer diameter improved the mass entrainment ratio as well. However, in comparison to the base mixer diameter of 3.25 mm, the EJ2 mass entrainment ratio improvement was only 0.1% for a mixer diameter of 3.35. The reduction in the mixer diameter to 3.15 mm resulted in a degradation of the mass entrainment ratio of up to approximately 2%.

The sensitivity analysis of the diffuser angle is presented in fig. 8 for EJ1 and EJ2. An increase in the diffuser angle resulted in a decreased velocity of the mixed fluid, thereby increasing the pressure of the fluid along the diffuser. Hence, the mass entrainment ratio increased with increasing diffuser angle. The largest improvement in the mass entrainment ratio was 20% for an EJ1 diffuser angle of 15°. The best ejector performance obtained for EJ2 was indicated for the same ejector diffuser angle as EJ1 of 15°, for which the mass entrainment ratio improved by up to 15%. However, the performance improvement obtained for EJ1 and EJ2 was similarly for a diffuser angle in the range of 10° to 15°. The increased diffuser angle directly led to shorter total lengths of the liquid ejector. Hence, the increase in the diffuser angle from 5° to 10° indicated the high ejector performance improvement, and the subsequent increase was not necessary.



**Figure 6. Mass entrainment ratio vs. mixer length for EJ1 and EJ2**



**Figure 7. Mass entrainment ratio vs. mixer diameter for EJ1 and EJ2**

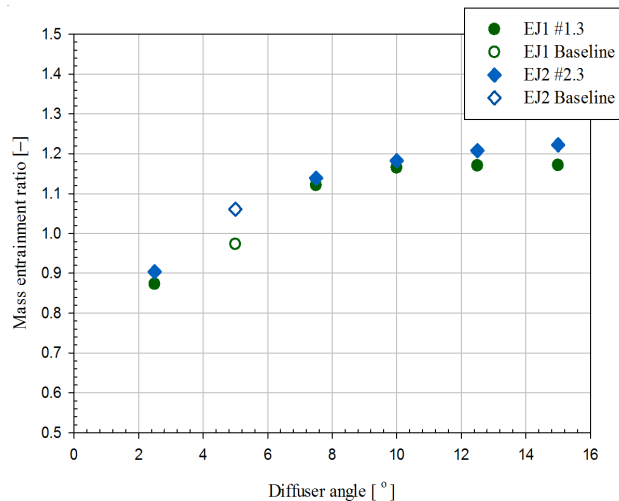


**Figure 8.** Mass entrainment ratio vs. diffuser angle for EJ1 and EJ2

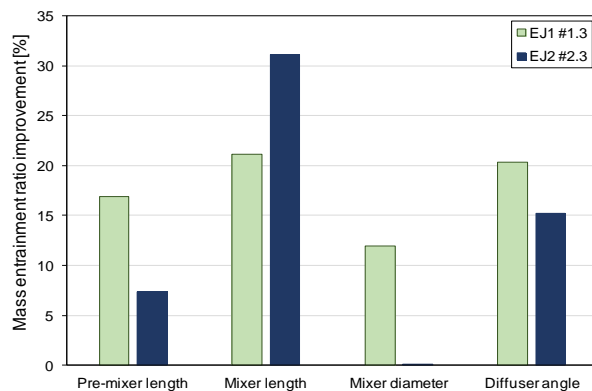


**Figure 9.** The best mass entrainment ratio for the parameterised liquid ejector dimensions

distributions was performed. Finally, a sensitivity analysis of the pre-mixer length, the mixer length and diameter, and the diffuser angle of both liquid ejectors was presented.

The validation procedure indicated a motive mass flow rate average discrepancy of approximately 11% and approximately 5% for EJ1 and EJ2, respectively. The average discrepancy of the EJ1 suction mass flow rate was 10%, and that of the EJ2 suction mass flow rate was 3%, thereby demonstrating the high accuracy of the CFD results. The distributions of the liquid ejector pressure, vapour quality and Mach number demonstrated the strong influence of the pre-mixing and mixing section geometry on the liquid ejector performance. The shockwaves of the motive flow influenced the pressure of the mixed flow in the pre-mixing section.

The parameterisation process resulting in the reduction of the pre-mixer length and mixer length improved the mass entrainment ratio of both liquid ejectors. Moreover, the increased diffuser angle and mixer diameter improved the performance of the liquid ejector. In

Based on the previous results, the best mass entrainment ratio improvement of the selected parameterised parameters is shown in fig. 9. The comparison was prepared for both investigated ejectors. The highest improvement of the mass entrainment ratio of EJ1 was obtained for the decreased mixer length and for the increased diffuser angle. EJ2 obtained the highest mass entrainment ratio for the decreased mixer length, which significantly improved the liquid ejector performance. Note that the increased diffuser angle improved the mass entrainment ratio by over 15% for both ejectors.

## Conclusions

Two configurations of R744 liquid ejectors were numerically investigated. The homogenous equilibrium model was employed because it provided a relatively high accuracy when the inlet motive nozzle parameters were not greatly dissimilar to those at the critical point. The validation of the numerical results was performed based on the experimental results obtained by the authors at the SINTEF Energy Research Laboratory. An analysis of the specific ejector parameter distributions was performed.

the sensitivity analysis, the highest mass entrainment ratio improvement of 21% was obtained for EJ1 with the shorter mixer length. In addition, the wider angle of the EJ1 diffuser improved the mass entrainment ratio by up to 20%. For EJ2, the shorter mixer length resulted in the best mass entrainment ratio improvement of 31%. The increased diffuser angle improved the liquid ejector performance by up to 15% and led to a reduced ejector length. These results showed that the liquid ejector performance is dependent on different geometrical parameters than that of the vapour ejector.

### Acknowledgment

The authors gratefully acknowledge the financial support of the Polish Norwegian Research Fund through project No. Pol-Nor/196445/29/2013 and partially The Research Council of Norway through project No. 244009/E20.

### References

- [1] Deng, J. Q., *et al.*, Particular Characteristics of Transcritical CO<sub>2</sub> Refrigeration Cycle with an Ejector, *Applied Thermal Engineering*, 27 (2007), 2-3, pp. 381-388
- [2] Elbel, S., Historical and Present Developments of Ejector Refrigeration Systems with Emphasis on Transcritical Carbon Dioxide Air-Conditioning Applications, *Inter. Jour. of Refrig.-Revue Internationale Du Froid*, 34 (2011), 7, pp. 1545-1561
- [3] Elbel, S., Hrnjak, P., Experimental Validation of a Prototype Ejector Designed to Reduce Throttling Losses Encountered in Transcritical R744 System Operation, *International Journal of Refrigeration-Revue Internationale Du Froid*, 31 (2008), 3, pp. 411-422
- [4] Hafner, A., *et al.*, Multi-Ejector Concept for R-744 Supermarket Refrigeration, *Inter. Jour. of Refrig.-Revue Internationale du Froid*, 43 (2014), July, pp. 1-13
- [5] Li, D., Groll, E. A., Transcritical CO<sub>2</sub> Refrigeration Cycle with Ejector-expansion Device, *Inter. Jour. of Refrig.*, 28 (2005), 5, pp. 766-773
- [6] Sumeru, K., *et al.*, A Review on Two-phase Ejector as an Expansion Device in Vapor Compression Refrigeration Cycle, *Renewable & Sustainable Energy Reviews*, 16 (2012), 7, pp. 4927-4937
- [7] Li, Y., *et al.*, Experimental Evaluation of an Ejector as Liquid Re-circulator in a Falling-film Water Chiller, *International Journal of Refrigeration*, 40 (2014), Apr., pp. 309-316
- [8] Dopazo, J. A., Fernandez-Seara, J., Experimental Evaluation of an Ejector as Liquid Re-circulator in an Overfeed NH<sub>3</sub> System with a Plate Evaporator, *Inter. Jour. of Refrig.*, 34 (2011), 7, pp. 1676-1683
- [9] Giroto, S., CO<sub>2</sub> Refrigeration System for Warm Climates, Enex srl, Padernello di Paese, 2013, [http://www.enex-ref.com/download/Enjector\\_promo\\_eng.pdf](http://www.enex-ref.com/download/Enjector_promo_eng.pdf)
- [10] Giroto, S., Benefits with Enjector, Enex srl, Padernello di Paese, 2013, [http://www.enexref.com/download/Enjector\\_promo\\_eng.pdf](http://www.enexref.com/download/Enjector_promo_eng.pdf)
- [11] Banasiak, K., *et al.*, Development and Performance Mapping of a Multi-ejector Expansion Work Recovery Pack for R744 Vapour Compression Units, *Inter. Jour. of Refrig.*, 57 (2015), Sep., pp. 265-276
- [12] Smolka, J., *et al.*, A Computational Model of a Transcritical R744 Ejector Based on a Homogeneous Real Fluid Approach, *Applied Mathematical Modelling*, 37 (2013), 3, pp. 1208-1224
- [13] Palacz, M., *et al.*, Application Range of the HEM Approach for CO<sub>2</sub> Expansion Inside Two-phase Ejectors for Supermarket Refrigeration Systems, *Inter. Jour. of Refrig.*, 59 (2015), Nov., pp. 251-258
- [14] Hafner, A., *et al.*, R744 Refrigeration System Configurations for Supermarkets in Warm Climates, 3<sup>rd</sup> IIR International Conference on Sustainability and the Cold Chain, ICCO 2014, International Institute of Refrigeration, 2014
- [15] Lemmon, E. W., *et al.*, M.O., NIST Standard Reference Database 23: Reference Fluid Thermodynamic and Transport Properties-REFPROP, Standard Reference Data Program, 2013

Paper submitted: December 10, 2015

Paper revised: March 2, 2016

Paper accepted: April 6, 2016